MOLECULAR AND CELLULAR BIOLOGY, June 2009, p. 3266–3279 Vol. 29, No. 12
0270-7306/09/$08.00+0 doi:10.1128/MCB.00064-09


# Fas-Mediated Apoptosis Is Regulated by the Extracellular Matrix Protein CCN1 (CYR61) In Vitro and In Vivo[▽]

Vladislava Juric, Chih-Chiun Chen, and Lester F. Lau*

*Department of Biochemistry and Molecular Genetics, University of Illinois at Chicago, 900 S. Ashland Avenue, Chicago, Illinois 60607*

Received 14 January 2009/Returned for modification 20 February 2009/Accepted 6 April 2009

**Although Fas ligand (FasL) is primarily expressed by lymphoid cells, its receptor Fas (CD95/Apo-1) is broadly expressed in numerous nonlymphoid tissues and can mediate apoptosis of parenchymal cells upon injury and infiltration of inflammatory cells. Here we show that CCN1 (CYR61) and CCN2 (CTGF), matricellular proteins upregulated at sites of inflammation and wound repair, synergize with FasL to induce apoptosis by elevating cellular levels of reactive oxygen species (ROS). CCN1 acts through engagement of integrin $\alpha_6\beta_1$ and cell surface heparan sulfate proteoglycans, leading to ROS-dependent hyperactivation of p38 mitogen-activated protein kinase in the presence of FasL to enhance mitochondrial cytochrome *c* release. We show that CCN1 activates neutral sphingomyelinase, which functions as a key source of CCN1-induced ROS critical for synergism with FasL. Furthermore, Fas-dependent hepatic apoptosis induced by an agonistic monoclonal anti-Fas antibody or intragastric administration of alcohol is severely blunted in knock-in mice expressing an apoptosis-defective *Ccn1* allele. These results demonstrate that CCN1 is a physiologic regulator of Fas-mediated apoptosis and that the extracellular matrix microenvironment can modulate Fas-dependent apoptosis through CCN1 expression.**

Cell adhesion to several abundant extracellular matrix (ECM) proteins via engagement of integrin receptors is known to induce potent prosurvival signals, whereas detachment from the ECM triggers many cell types to undergo anoikis, a form of apoptotic cell death (13). This regulation of cell survival through integrin-mediated cell adhesion plays a critical role in controlling homeostasis and the integrity of tissue architecture, whereas unligated or inappropriately ligated integrins may elicit apoptotic signals (12). However, during embryogenesis, inflammation, tissue remodeling, and wound repair, death-inducing factors can provoke programmed or apoptotic death in normal cells without requiring their detachment from the ECM (4).

Fas (CD95/APO-1) is a member of the tumor necrosis factor (TNF) receptor family of cell surface death receptors that mediates apoptotic signals upon binding to its specific ligand, FasL. Ligation of Fas to FasL or its agonistic antibodies results in receptor clustering, recruitment of the adaptor protein FADD, and activation of the proteolytic caspase cascade (19, 50). Whereas FasL is primarily expressed in activated T lymphocytes, natural killer cells, and tissues of immune privilege, Fas is broadly expressed in most lymphoid and nonlymphoid tissues (50). Fas-mediated apoptosis is critical for the regulation of the immune response, including deletion of activated T and B lymphocytes, cell death-inducing activity of cytotoxic T cells, and removal of infiltrating lymphocytes in immune-privileged tissues (19, 50). Fas also plays an important role in parenchymal cell apoptosis in many organs during tissue injury and upon inflammatory infiltration of lymphocytes (7, 20, 38, 42, 46). Consistent with the notion that cell adhesion promotes cell survival, integrin-matrix interactions inhibit Fas-dependent apoptosis in a variety of cell types (22, 32). Thus, optimal apoptotic responses to Fas/FasL signaling in adherent parenchymal cells must override the cytoprotective effects of integrin-mediated cell adhesion. In these instances, dynamic changes in the ECM induced by inflammation or injury repair may establish conditions that are permissive of, or conducive to, the apoptotic responses to FasL.

Recent studies have described the emergence of ECM proteins that can induce or promote apoptosis (49, 60, 65). Among them are members of the CCN family (9), which are secreted cysteine-rich proteins that serve regulatory rather than structural roles in the ECM and are therefore considered matricellular proteins (6). CCN1 (CYR61) and CCN2 (CTGF) support cell adhesion, stimulate cell migration, induce angiogenesis, and promote chondrogenic differentiation, exerting their functions primarily through direct binding to integrin receptors. CCN1 and CCN2 promote the survival of endothelial cells through integrin $\alpha_v\beta_3$ but induce apoptosis in p21-deficient fibroblasts through $\alpha_6\beta_1$ via a caspase-8-independent mechanism (3, 40, 60). CCN1 and CCN2 are also critical for embryonic development, as *Ccn1*-null mice die during midgestation due to cardiovascular abnormalities and *Ccn2*-deficient mice perish perinatally as a consequence of severe skeletal malformations (29, 47, 48). In the adult, CCN proteins are highly expressed at sites of inflammation, injury repair, and tissue remodeling and are implicated in diseases where inflammation plays a role, including fibrosis, atherosclerosis, arthritis, and cancer (9). Furthermore, the presence of CCN1 in the ECM enables TNF-α to induce apoptotic death in normal cells without inhibition of NF-κB signaling or de novo protein synthesis, conditions thought to be necessary for TNF-α to be cytotoxic (10).

* Corresponding author. Mailing address: Department of Biochemistry and Molecular Genetics, University of Illinois at Chicago College of Medicine, Chicago, IL 60607. Phone: (312) 996-6978. Fax: (312) 996-7034. E-mail: LFLau@uic.edu.

▽ Published ahead of print on 13 April 2009.

Here we show that CCN1 and CCN2 can synergize with FasL and significantly enhance FasL-induced apoptosis in fibroblasts. Mechanistically, CCN1 engages integrin $\alpha_6\beta_1$ and cell surface heparan sulfate proteoglycans (HSPGs), leading to the reactive oxygen species (ROS)-dependent hyperactivation of p38 mitogen-activated protein kinase (MAPK) in the presence of FasL, which greatly enhances mitochondrial cytochrome *c* release and apoptosis. We show that CCN1 is a novel activator of neutral sphingomyelinase (nSMase), which is an essential contributor to CCN1-induced ROS. Further, Fas-dependent hepatic cell death is greatly diminished in knock-in mice expressing an apoptosis-defective mutant of CCN1 that is unable to bind $\alpha_6\beta_1$-HSPGs. Together, these results show that CCN1 is a physiologic regulator of Fas-mediated apoptosis and indicate that Fas-dependent cell death at sites of inflammation and injury repair may be controlled by the matrix microenvironment through CCN1 expression.

## MATERIALS AND METHODS

**Cell culture.** Normal human skin fibroblasts (HSFs) were obtained from the American Type Culture Collection, maintained at 37°C and 5% $CO_2$ in Iscove's modified Dulbecco's medium (Invitrogen) with 10% fetal bovine serum (FBS; HyClone), and used before reaching 20 population doublings.

**Proteins, reagents, and antibodies.** Recombinant CCN1 and CCN2 and mutant proteins (DM, TM, D125A) were produced and purified from a baculovirus expression system in Sf9 insect cells as described previously (11, 39). Human trimeric Fas ligand was from Axxora. Human fibronectin (FN), vitronectin (VN), mouse laminin, rat type 1 collagen (Col I), anti-Bax (6A7), anti-cytochrome *c* (6H2.B4) for immunofluorescence, and anti-Fas (Jo2 and DX2) were from BD Biosciences. Caspase-8-, caspase-9-, and caspase-3-inhibitory peptides (*N*-benzyloxycarbonyl-IETD-fluoromethyl ketone [Z-IETD-FMK], Z-LEHD-FMK, and Z-DEVD-FMK, respectively), SB202190, SB203580, and SP600125 were from Calbiochem, and the caspase-10 inhibitor (Z-AEVD-FMK) was from R&D Systems. Caspase-10 chromogenic substrate *N*-acetyl-AEVD-*p*-nitroanilide (Ac-AEVD-pNA) was from AnaSpec. Antibodies for caspase-8 and phospho-c-Jun N-terminal protein kinase 1/2 (phospho-JNK1/2; Thr183/Tyr185) were from Assay Designs, those for caspase-9, -3, phospho-p38 MAPK (Thr180/182), phospho-c-Jun (Ser63), and JNK1/2 were from Cell Signaling Technology, and those for p38 MAPK, Fas (C-20), and poly(ADP ribose) polymerase (PARP; H-250) were from Santa Cruz. Cytochrome *c* and cytochrome *c* oxidase 4 antibodies for immunoblots were from Clontech. Mouse monoclonal anti-β-actin antibody (AC-15), GW4869, and desipramine were from Sigma. Function-blocking monoclonal antibodies (MAbs) against integrins $\alpha_6$ (GoH3) and $\alpha_v\beta_5$ (P1F6) were from Chemicon, and anti-VNRI (anti-$\alpha_v\beta_3$) was a generous gift from S. C. Lam. CM-$H_2$DCFDA [5- (and 6-)chloromethyl-2′,7′-dichlorodihydrofluorescein diacetate acetyl ester), DHC (dihydrocalcein), and DHE (dihydroethidium) were from Invitrogen. Phosphatidylserine, porcine brain sphingomyelin, and ceramide were from Avanti Polar Lipids. Choline-[*methyl*-$^{14}$C]sphingomyelin was from PerkinElmer.

**Apoptosis assays.** Non-tissue culture plates were coated by overnight incubation at 4°C with rat tail Col I (5 μg/ml), VN (3 μg/ml), FN (1 μg/ml), CCN1 (2 μg/ml), or CCN2 (2 μg/ml), onto which serum-starved HSFs were plated and allowed to attach for 20 min in Iscove's modified Dulbecco's medium supplemented with 0.1% bovine serum albumin (BSA). Cells were treated with FasL, and apoptosis was assessed either by TUNEL assay (ApopTag Red in situ apoptosis detection kit; Millipore) using the manufacturer's protocol or by DAPI (4′,6-diamidino-2-phenylindole) staining (45). Briefly, incubation of cells with apoptosis-inducing factors was terminated by addition of 10% formaldehyde to the culture medium and fixation overnight at room temperature (RT). Fixed cells were rinsed once with phosphate-buffered saline (PBS) and stained with 1 mg/ml DAPI for 5 min at RT. Apoptotic cells were counted in 10 randomly selected high-power fields (Nikon Optiphot). This method gives results comparable to those obtained by terminal deoxynucleotidyltransferase-mediated dUTP-biotin nick end labeling (TUNEL). Data are presented as mean % apoptosis ± standard deviations (SD) from experiments done in triplicate. All apoptosis assays were done at least three times with similar results.

**Annexin V-PI staining and flow cytometry analysis.** Briefly, $3 \times 10^5$ cells were treated as noted in the figure legends, harvested, and rinsed twice with binding buffer (10 mM HEPES-NaOH [pH 7.4], 140 mM NaCl, 2.5 mM $CaCl_2$). Staining with annexin V-fluorescein isothiocyanate (FITC) and propidium iodide (PI) was done with annexin V-FITC apoptosis detection kit I (BD Biosciences) by following the manufacturer's protocol.

**Immunoblotting and immunocytochemistry.** Immunoblotting was done by standard methods after electrophoretic separation of proteins by 10% sodium dodecyl sulfate-polyacrylamide gel electrophoresis. To detect cytochrome *c* release, cells were treated as described in the figure legends and cytosolic extracts were prepared and analyzed as described previously (45). For immunocytochemistry, cells were grown on chamber slides, treated as noted in the figure legends, and probed with anti-cytochrome *c* (6H2.B4 clone) or monoclonal anti-Bax (6A7 clone). Images were acquired with a Zeiss Axiovert 200 M microscope with an AxioCam MRc5 camera (AxioVision Rel 4.6 software).

**In vitro caspase activity assay.** Caspase-10 activity was measured by using a modification of a published protocol (26). Briefly, cells were lysed in hypotonic buffer (10 mM HEPES [pH 7.4], 50 mM NaCl, 2 mM $MgCl_2$, 5 mM EGTA, 1 mM phenylmethylsulfonyl fluoride, and protease inhibitor cocktail). After incubation on ice for 15 min and four freeze-thaw cycles, lysates were spun at $10{,}000 \times g$ for 1 min at 4°C, and protein concentration in supernatants containing the cytosolic fraction was measured with a Bio-Rad Dc protein assay kit. Extracts containing 40 μg total protein were diluted with an equal volume of 2× reaction buffer (50 mM HEPES [pH 7.4], 0.2% CHAPS {3-[(3-cholamidopropyl)-dimethylammonio]-1-propanesulfonate}, 20% glycerol, 2 mM EDTA, 10 mM dithiothreitol), and caspase-10 chromogenic substrate (Ac-AEVD-pNA) was added to a final 200 μM concentration. The caspase-10 inhibitor Ac-AEVD-FMK (50 μM) was added to demonstrate the specificity of the assay. The absorbance of cleaved substrate at 420 nm was measured with the Labsystem Multiskan MS plate reader.

**Cell surface expression of Fas.** Cells were harvested using 5 mM EDTA in PBS, rinsed, and without permeabilization incubated with FITC-conjugated anti-Fas (DX2; 10 μg/ml) or FITC-conjugated control immunoglobulin G (IgG) in blocking solution (1% normal goat serum, 0.02% $NaN_3$ in PBS). After 40 min of incubation on ice, cells were rinsed and fixed in 1% paraformaldehyde in PBS, pH 7.4, and $10^5$ cells/sample were analyzed by flow cytometry (Cell Lab Quanta SC MPL; Beckman Coulter). Histogram overlays were generated in Summit V31 software (Cytomation, Inc.).

**ROS measurements.** Hydrogen peroxide and superoxide species in live cells were detected with indicator dyes CM-$H_2$DCFDA and DHE, respectively, by flow cytometry (62). Cells were loaded with the indicator dye (5 μM) for 15 min at 37°C, followed by 10 min of incubation with CCN1, CCN2, or FasL. After being rinsed, cells were harvested and resuspended to $0.2 \times 10^6$ cells/ml in cold PBS containing 5% FBS. Fluorescence from $10^5$ cells per sample was analyzed by flow cytometry (Cell Lab Quanta SC MPL; Beckman Coulter). Data collected from triplicate samples were plotted against geometric mean fluorescence intensities or presented as histograms generated by Summit V31 software. For detection of ROS by fluorescence microscopy (Leica; model DM IRB) (2), cells were loaded with 10 μM DHC and counterstained with Hoechst 33342. Five random high-power fields per condition were photographed with a QImaging Retiga 2000R camera, and integrated DHC fluorescence intensities were measured with ImageJ 1.36b software (NIH).

**siRNA and semiquantitative RT-PCR.** HSFs were transfected using Lipofectamine 2000 reagent (Invitrogen) with 50 nM siGENOME SMARTpool small interfering RNA (siRNA) against nSMase1 (NM_003080), siRNA against p38α (sense: CCUACAGAGAACUGCGGUU-dTdT) (30), or control nontargeting siRNA (Dharmacon). nSMase1 gene silencing was confirmed 72 h posttransfection by semiquantitative reverse transcription-PCR (RT-PCR) analysis. Total RNA was isolated with Tri reagent (Molecular Research Center, Inc.). nSMase1-specific primers (forward, 5′-CAACAAGTGTAACGACGATGCC-3′; reverse, 5′-CGATTCTTTGGTCCTGAGGTGT-3′) and GAPDH (glyceraldehyde-3-phosphate dehydrogenase) primers (forward, 5′-ATCGTGGAAGGACTCATG ACCACA-3′; reverse, 5′-CCTGCTTCACCACCTTCTTGATGT-3′) were used in RT-PCR to confirm downregulation.

**Constructs and CCN1 and Bcl2 overexpression.** Human *CCN1* cDNA was cloned into pCMV-Script vector (Stratagene) using XmaI and HindIII cloning sites and was confirmed by sequencing analysis. HSFs grown in 35-mm dishes until 80% confluent were transfected with 1 μg/ml empty vector or the pCMV-CCN1 expression construct using Lipofectamine 2000 (Invitrogen). nSMase assays or ceramide measurements were done 24 h posttransfection. pBabe-eGFP and pBabe-eGFP-BCL2 constructs were a kind gift from Nissim Hay. HSFs were transiently transfected with 1 μg/ml plasmid using Lipofectamine 2000, and overexpression was confirmed by immunoblot analysis after 24 h. To assess the effect of Bcl-2 overexpression on CCN1/FasL apoptosis, transfected cells were treated with CCN1 and/or FasL for 5 h and the apoptotic index in green fluo-

rescent protein (GFP)-positive cells was determined by fluorescence microscopy. At least 50 GFP-positive cells per treatment were assessed for apoptosis in experiments done in triplicate.

**In vitro nSMase assay.** The activity assay specific for nSMase was conducted in neutral pH that is nonpermissive for acidic SMase (aSMase) activity (66). Cells were lysed in a buffer containing 20 mM HEPES (pH 7.4), 10 mM $MgCl_2$, 2 mM EDTA, 1 mM dithiothreitol, 0.1 mM $Na_3VO_4$, 10 mM β-glycerophosphate, 750 μM ATP, 1 mM phenylmethylsulfonyl fluoride, protease inhibitor cocktail, and 0.1% Triton X-100 by 15 min of incubation on ice. After a brief sonication, lysates were centrifuged at 14,000 × *g* and 4°C for 10 min. Protein concentration in supernatants containing cytosolic and membrane fractions was determined by Dc assay (Bio-Rad). Samples containing 30 to 50 μg of total protein (in a 50-μl volume) were incubated with an equal volume of a buffer containing 20 mM HEPES (pH 7.4), 1 mM $MgCl_2$, 6.7% phosphatidylserine, and 100 μM choline-[*methyl*-$^{14}$C]sphingomyelin (10 cpm/pmol, 50 nCi/reaction). The reaction was stopped after 2 h of incubation at 37°C by adding 0.25 ml of $H_2O$ and 0.8 ml chloroform-methanol (2:1 [vol/vol]). After vortexing and phase separation at 1,500 × *g* for 5 min, the aqueous phase was removed and radioactivity was measured with a liquid scintillation counter (Beckman Coulter).

**Ceramide quantitation.** Lipids were extracted from HSFs according to the Bligh and Dyer method (5), and ceramide was measured by the diacylglycerol kinase assay, which uses recombinant *Escherichia coli* diacylglycerol kinase, which phosphorylates diacylglycerols and ceramides in lipid extracts (56). After the reaction was carried out in the presence of [γ-$^{32}$P]ATP, lipids were separated by thin-layer chromatography, and thin-layer chromatography plates were exposed to X-ray film. Bands corresponding to the $R_f$ value for ceramides were quantified by densitometry. The amount of ceramide in cells was calculated after comparison with ceramide standards, and results were expressed as pmol ceramide per $10^5$ cells.

**Bax immunofluorescence.** Mitochondria were labeled by adding 80 nM Mito-Tracker Orange CMTMRos to the culture medium for 10 min at 37°C and 5% $CO_2$. Cells were fixed with 2% paraformaldehyde, pH 7.5, for 15 min at RT. After five rinses with PBS, cells were permeabilized for 30 min at RT in 0.5% CHAPS, which does not induce an activating conformational change in Bax protein, which nonionic detergents are known to do (28). After 1 h of blocking in 2% normal goat serum and 3% BSA in PBS, cells were labeled with 5 μg/ml anti-Bax (6A7 clone) by overnight incubation at 4°C. After staining with Alexa Fluor 488-conjugated secondary antibody and counterstaining with DAPI, samples were mounted with Fluoromount G and images were acquired on Zeiss Axiovert 200 M microscope with an AxioCam MRc camera.

**Animals and MEFs.** The animal protocols were approved by the Animal Care Committee of the University of Illinois at Chicago. Two independent lines of *Ccn1*$^{dm/dm}$ mice were generated in an svJ129-C57BL/6 mix background and backcrossed a minimum of six times into the C57BL/6 background (10). MEFs were harvested from embryonic day 12.5 embryos according to standard procedures, and experiments were performed no later than passage 3.

**Liver injury models.** *Ccn1*$^{wt/wt}$ and *Ccn1*$^{dm/dm}$ male mice between 8 and 10 weeks old were treated with agonistic Fas antibody (Jo2 clone, endotoxin and azide free) or control IgG at 0.5 μg/g body weight via tail vein injection (52). Mice were sacrificed 2 h thereafter, and livers were paraffin embedded. Sections (7 μm thick) were assayed for apoptosis by TUNEL, and positive nuclei were counted in five random fields (200× magnification). Serum alanine aminotransferase (ALT) activities were measured 4 h after intraperitoneal delivery of Jo2 (0.5 μg/g body weight) with the Hitachi 912 automated analyzer. For alcohol-induced liver injury, a binge drinking model was used (70). Male mice were fed intragastrically with alcohol at a dose of 2 g/kg body weight, delivered by a single gavage of 32% (vol/vol) ethanol, and sacrificed 24 h later. Liver tissue was processed for histological analysis and TUNEL staining. Images were acquired with a Zeiss Axiovert 200 M microscope with the AxioCam MRc5 camera (AxioVision Rel 4.6 software). Apoptosis was quantified as described above.

**Statistical analysis.** Each experiment in this study was repeated at least three times with similar results; the results of one representative experiment done in triplicate are shown, and data are presented as means ± SD. Student's *t* test was employed to calculate *P* values.

## RESULTS

**CCN1 and CCN2 synergize with FasL to induce apoptosis.** To test the hypothesis that FasL-induced apoptosis may be modulated by the ECM microenvironment, we plated serum-starved HSFs on surfaces coated with various ECM proteins, including Col I, VN, FN, CCN1, and CCN2. These CCN proteins support cell adhesion and cell spreading and induce adhesive signaling, including activation of focal adhesion kinase, paxillin, and Rac (8). Cells were either left untreated or incubated with FasL, and apoptosis was monitored by TUNEL assay (Fig. 1A). TUNEL-positive cells also showed nuclear condensation, as indicated by DAPI staining, consistent with apoptotic cell death (17). Cells adhered on purified CCN1 or CCN2 exhibited a significantly higher apoptotic index than those adhered on other ECM proteins in the presence of FasL, although cell adhesion on CCN proteins per se did not induce apoptosis under these conditions. Within 5 h of FasL treatment, ~80% of cells adhered on CCN1 or CCN2 were apoptotic, whereas only ~35% of cells adhered on other ECM proteins were undergoing apoptosis, as revealed by DAPI staining (Fig. 1B). CCN1 also synergized with FasL when added as a soluble factor to cells adhered on tissue culture dishes, as shown by flow cytometric analysis after annexin V-PI staining (Fig. 1C). In addition, CCN1 synergized with FasL in a dose-dependent manner (Fig. 1D). Apoptosis in response to FasL was greatly reduced (to 2 to 3%) when cells were grown in medium containing 10% FBS (Fig. 1E), reflecting a protective effect of serum against FasL-induced apoptosis (57). Nevertheless, CCN1 enhances FasL cytotoxicity even in the presence of 10% serum, despite the antiapoptotic effects of serum growth factors.

**CCN1 synergizes with FasL through integrin $\alpha_6\beta_1$ and HSPGs.** CCN proteins are known to elicit various cellular responses through direct binding to distinct integrin receptors, and the specific integrins utilized are dependent on the cell type and context (36). In HSFs, CCN1 binds integrins $\alpha_6\beta_1$, $\alpha_v\beta_5$, and $\alpha_v\beta_3$ to regulate aspects of cell behavior including cell adhesion, migration, and DNA synthesis, respectively, with $\alpha_6\beta_1$ acting with cell surface HSPGs as a coreceptor (9). To identify the CCN1 receptors required for its synergism with FasL, we tested the effects of function-blocking MAbs against the known integrin receptors for CCN1. Pretreatment of cells with anti-$\alpha_6$ MAb (GoH3) abolished CCN1/FasL synergism, whereas control IgG had no effect (Fig. 2A). The addition of soluble heparin to the culture medium eliminated the effect of CCN1, most likely by saturating the heparin-binding sites of CCN1 and thus preventing its interaction with cell surface HSPGs (Fig. 2B). By contrast, function-blocking MAbs against integrins $\alpha_v\beta_3$ and $\alpha_v\beta_5$, alone or in combination, did not inhibit CCN1/FasL synergism (Fig. 2C). These results are consistent with the interpretation that CCN1 interaction with $\alpha_6\beta_1$-HSPGs is crucial for its synergism with FasL. To test this notion further, we examined the effects of CCN1 mutants that are unable to bind specific integrins. In accord with antibody-blocking results, the CCN1 mutants DM and TM, which are defective for binding $\alpha_6\beta_1$-HSPG (39), were completely unable to enhance FasL-induced apoptosis (Fig. 2D). By contrast, the integrin $\alpha_v$-binding-defective CCN1 mutant, D125A (11), was still capable of synergizing with FasL (Fig. 2D). Together, these results show that CCN1 functions to augment FasL-induced apoptosis primarily through engagement of integrin $\alpha_6\beta_1$ and HSPGs.

**CCN1 amplifies the Fas-induced caspase cascade without altering Fas expression or cell surface localization.** In some cell types, Fas receptor complexes activate a sufficient amount

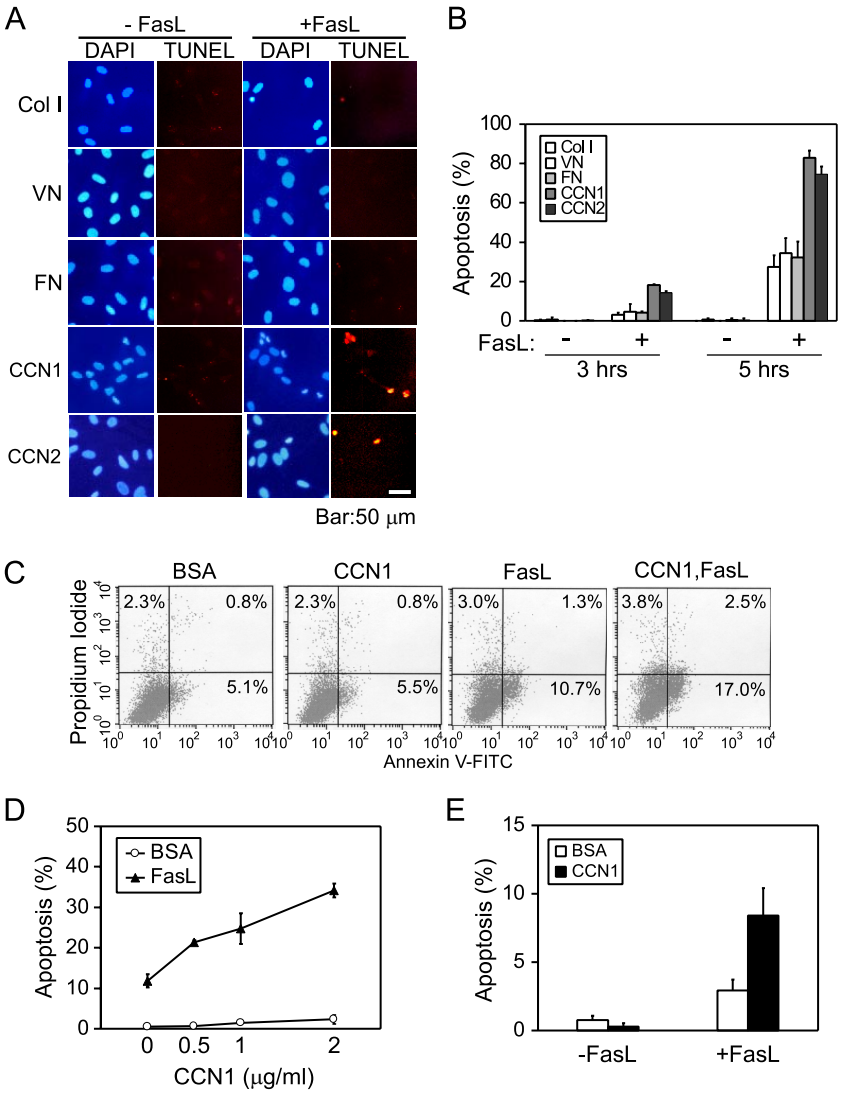


FIG. 1. CCN1 and CCN2 synergize with FasL to induce apoptosis. (A) Serum-starved HSFs were adhered to dishes precoated with Col I, VN, FN, CCN1, or CCN2 in serum-free medium. Cells were untreated or treated with FasL (50 ng/ml) at 37°C for 3 h, and apoptosis was detected by a TUNEL assay. TUNEL-positive nuclei (red) appear condensed, as shown by DAPI counterstaining. (B) Cells adhered to various matrix proteins were either untreated or stimulated with FasL, and apoptosis was scored 3 and 5 h thereafter by DAPI staining. (C) Serum-starved HSFs adherent to tissue culture dishes were treated with various factors added to the culture medium and harvested after 4 h. After HSFs were double-stained with annexin V-FITC and PI, cell death was assessed by flow cytometry. Results are shown as a bivariate distribution of annexin V-FITC and PI fluorescence. Cells in the lower left quadrants were defined as viable (double negative), those in the lower right quadrants as early apoptotic (annexin V positive, PI negative), those in the upper left quadrants as necrotic (PI positive, annexin V negative), and those in the upper right quadrants as late apoptotic (double positive). Percentages of cells in all quadrants except the lower left are shown. (D) Apoptosis in response to increasing amounts of soluble CCN1 in the presence of FasL (100 ng/ml) was quantified after 4 h of treatment. (E) Apoptosis was induced by treatment of cells with FasL (200 ng/ml) and/or CCN1 (1 μg/ml) in medium containing 10% FBS and quantified after 6 h.

of the initiator caspase-8 to trigger apoptosis through direct activation of the executioner caspase-3, whereas in other cell types the apoptotic signals must be amplified through mitochondrial cytochrome *c* release facilitated by caspase-8 cleavage of the BH-3-containing protein Bid (41). Cytoplasmic cytochrome *c* forms the apoptosome with Apaf-1 to activate caspase-9, which in turn activates caspase-3 and triggers apoptosis. Treatment of HSFs with inhibitory peptides for caspase-8, -10, -9, or -3 completely abolished Fas-induced apoptosis either in the presence or absence of CCN1, indicating that caspases are required for both FasL- and CCN1/FasL-dependent apoptosis (Fig. 3A). We then monitored the activation of caspase-8, -9, and -3 by cleavage of their proenzymes and the activity of caspase-10 by hydrolysis of the caspase-10-specific chromogenic substrate, Ac-AEVD-pNA (Fig. 3B to D). In each case, CCN1 by itself did not activate any of these caspases but greatly enhanced their activation in the presence of FasL.

Since CCN1 amplified the FasL-induced caspase cascade, we tested the possibility that it might enhance Fas receptor expression or cell surface localization. Pretreatment of cells with cycloheximide or anisomycin (AN) increased apoptosis

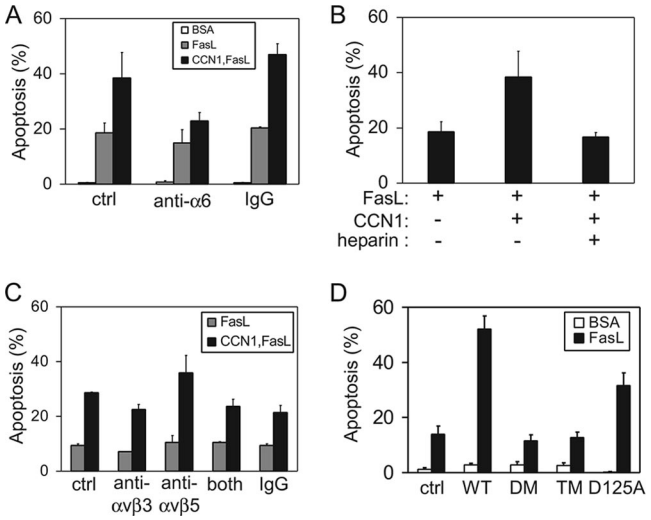


FIG. 2. Integrin $\alpha_6\beta_1$ and cell surface HSPGs are required for CCN1/FasL synergism. Apoptosis of HSFs treated as described below was quantified by DAPI staining after 4 h of incubation. (A) Anti-integrin $\alpha_6$ rat MAb (GoH3) or normal rat IgG (50 μg/ml each) was preincubated with HSFs 30 min prior to treatment with FasL with or without CCN1. (B) Soluble heparin (10 μg/ml), CCN1, and FasL were added where indicated. (C) Cells were untreated (ctrl) or incubated with MAbs against $\alpha_v\beta_3$ and/or $\alpha_v\beta_5$ or normal IgG for 30 min before addition of FasL with or without CCN1. (D) Cells were treated with FasL and wild-type CCN1 (WT) or CCN1 mutant protein D125A (defective in binding integrin $\alpha_v$), DM, or TM (defective in binding integrin $\alpha_6\beta_1$-HSPG).

induced by FasL alone (Fig. 3E), most likely due to destabilization of the antiapoptotic protein FLIP, which inhibits activation of caspase-8 and -10 (57). However, CCN1 was still able to enhance FasL-induced cell death, showing that de novo protein synthesis is not required for CCN1/FasL synergism. Furthermore, the steady-state level of Fas protein was unchanged in cells treated with CCN1 and/or FasL, as judged by immunoblot analysis (Fig. 3F, top), indicating that CCN1 does not work by enhancing Fas synthesis or inhibiting Fas degradation. We then monitored cell surface localization of Fas by flow cytometry using an anti-Fas MAb, DX2. Treatment of cells with CCN1 and FasL, alone or in combination, had no effect on Fas localization on the cell surface (Fig. 3F, bottom, and data not shown). Therefore, CCN1 amplifies the Fas-dependent caspase cascade without regulating Fas expression or cell surface localization.

**CCN1 and CCN2 enhance FasL-induced apoptosis by elevating ROS.** Since ROS can mediate or augment Fas-induced apoptosis in some cell types (63), we investigated their potential role in CCN/FasL synergism. Although CCN1 has been shown to induce ROS through integrin signaling, no information is available on CCN2 in this regard (10). By loading cells with the indicator dye CM-$H_2$DCFDA, followed by flow cytometry, we found that both CCN1 and CCN2 were able to induce substantial accumulation of ROS (Fig. 4A and B). The ROS scavenger *N*-acetylcysteine (NAC) abrogated the synergism of CCN1 and CCN2 with FasL and partially inhibited FasL-induced apoptosis (Fig. 4C, top). Moreover, cotreatment of cells with CCN1 and FasL enhanced FasL-induced cleavage of the caspase-3 substrate PARP (59), an activity that was blocked by NAC (Fig. 4C, bottom). NAC blocked ROS accumulation and apoptosis concomitantly (Fig. 4C and D), consistent with the notion that intracellular ROS play an essential role in CCN/FasL synergism.

**nSMase1 is essential for CCN1-induced ROS accumulation and synergism with FasL.** Inflammatory cytokines, ionizing and UV irradiation, and anticancer drugs can activate SMases, which hydrolyze sphingomyelin into phosphocholine and the lipid messenger ceramide (34). Ceramide, in turn, can enhance cellular ROS levels by activation of NADPH oxidase, disruption of mitochondrial integrity, and/or downregulation of antioxidant enzymes (67). Since apoptotic signaling through Fas can activate SMase activity (15), we investigated whether SMases may play a role in Fas-mediated apoptosis in fibroblasts and in CCN1/FasL synergism. Two distinct forms of SMases are known: membrane-associated nSMase and a lysosomal aSMase, which functions only in acidic environments (16, 34). We found that GW4869, an inhibitor of nSMase, completely abrogated CCN1/FasL synergism but had no effect on apoptosis induced by FasL alone (Fig. 5A, top). By contrast, the aSMase inhibitor desipramine had no effect on apoptosis induced by FasL with or without CCN1, indicating that nSMase, but not aSMase, is specifically required for CCN1/FasL synergism. Moreover, the enhancement of FasL-induced PARP cleavage by CCN1 was blocked by GW4869 (Fig. 5A, bottom), providing a biochemical demonstration of the role of nSMase in CCN1/FasL synergism. Next we tested whether CCN1-induced ROS is dependent on nSMase activity. As shown by fluorescence microscopy following DHC staining, CCN1 treatment induced a large increase in cellular ROS levels, which was significantly reduced in the presence of GW4869 (Fig. 5B and C). These results show that nSMase is an important contributor to CCN1-induced ROS accumulation. It is interesting that treatment with both CCN1 and FasL results in less ROS accumulation than CCN1 alone (Fig. 4D and 5C), most likely because FasL can activate NF-κB, which induces antioxidant proteins such as Mn superoxide dismutase and ferritin heavy chain (35, 54). However, CCN1 and FasL induce more ROS accumulation than FasL alone (Fig. 5B), and this increased level of ROS is apparently sufficient to mediate the apoptotic synergism of CCN1.

Of the two known mammalian nSMases, nSMase1 (SMPD2) is ubiquitously expressed, whereas nSMase2 (SMPD3) is brain specific (16). Therefore, we targeted nSMase1 specifically by siRNA-mediated silencing to examine its role in apoptosis (Fig. 5D, top). Knockdown of nSMase1 abolished the synergism between CCN1 and FasL without blocking FasL-induced apoptosis (Fig. 5D, bottom), consistent with the effects of nSMase inhibition by GW4869 (Fig. 5A). These results show that nSMase1 is a critical mediator of CCN1-induced ROS accumulation and is essential for apoptosis induced by CCN1 and FasL, but not FasL alone.

**CCN1 activates nSMase and increases ceramide levels.** Since nSMase mediates ROS generation by CCN1, we assessed the ability of CCN1 to activate this class of enzymes using an assay specific for nSMase. Measuring nSMase activity in cell lysates at neutral pH, we found an ~80% increase in nSMase activity in cells transfected with a pCMV-CCN1 expression vector compared to control cells transfected with the empty vector (Fig. 5E). Moreover, the ceramide level in CCN1-over-

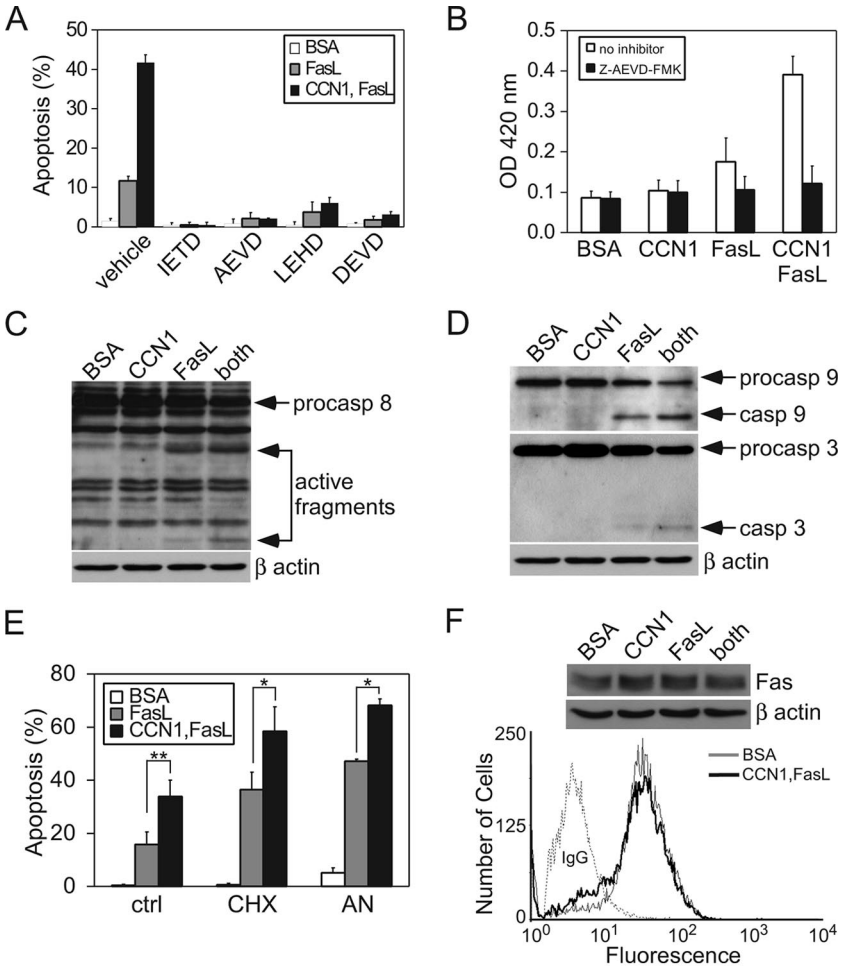


FIG. 3. CCN1 amplifies caspase activation by FasL without affecting the expression or cell surface localization of Fas. (A) HSFs were incubated with the vehicle (dimethyl sulfoxide) or inhibitory peptides against caspase-8, -10, -9, or -3 (Z-IETD-FMK, Z-AEVD-FMK, Z-LEHD-FMK, and Z-DEVD-FMK, respectively; 20 μM each) before treatment with FasL with or without CCN1. (B) Caspase-10 activity in lysates from cells treated with CCN1 and/or FasL was assayed using the chromogenic substrate Ac-AEVD-pNA in the presence or absence of the caspase-10 inhibitor (Z-AEVD-FMK). OD 420 nm, optical density at 420 nm. (C) Whole-cell lysates from cells treated as indicated for 4 h were immunoblotted with antibodies specific for caspase-8 or β-actin. The experiment was done at least three times with similar results. (D) Processing of caspase-9, and caspase-3 was detected by immunoblotting in lysates of cells treated as described above. The experiment was done at least three times with similar results. (E) Effects of cycloheximide (CHX) and anisomycin (AN) (10 μg/ml each) on apoptosis induction by CCN1 and/or FasL (*, $P < 0.01$; **, $P < 0.05$). (F, top) Lysates of cells treated as indicated were immunoblotted with anti-Fas (C-20) and β-actin antibodies. (Bottom) Cell surface expression of Fas was detected by flow cytometry. The histogram overlay shows staining with FITC-conjugated normal mouse IgG and anti-Fas MAb (DX2-FITC) in BSA-treated cells and in cells treated for 2.5 h with CCN1 and FasL.

expressing cells as measured by diacylglycerol kinase assay was ~70% higher than that in control cells (Fig. 5F). An increase in ceramide was also observed in HSFs after treatment with recombinant CCN1 protein (data not shown). These results show that CCN1 can activate nSMases and increase the cellular levels of ceramide.

**ROS-dependent hyperactivation of p38 MAPK mediates CCN1/FasL-induced cytochrome *c* release and apoptosis.** ROS are potent inhibitors of cellular phosphatases, and through this mechanism ROS can sustain the phosphorylation and activation of MAPKs, including JNK and p38 MAPKs (31, 37). We therefore analyzed the activation of MAPKs by FasL in the presence of CCN1. Inhibition of JNK activity by SP600125 did not block FasL-induced apoptosis with or without CCN1 (Fig. 6A, top), even though CCN1 was able to enhance the activation of JNK by FasL, as judged by JNK phosphorylation at Thr-183/Tyr-185 (Fig. 6B). SP600125 annihilated JNK-dependent phosphorylation of c-Jun at Ser-63 (Fig. 6C), demonstrating the efficacy of this JNK inhibitor. These results show that JNK is not required for CCN1/FasL synergism, in concordance with previous findings that JNK is dispensable for Fas-mediated apoptosis in lymphocytes (44). By contrast, the chemical blockers SB202190 and SB203580, which inhibit both p38α and p38β isoforms, significantly diminished FasL/CCN1-induced apoptosis (Fig. 6A, top). Similarly, SB203580 inhibited the synergistic processing of procapase-9 in the presence of CCN1 and FasL (Fig. 6A, bottom). Since HSFs express a high level of p38α and only a minimal amount of p38β, we investigated the specific role of p38α by siRNA silencing (30) (Fig. 6D, top). Indeed, depletion of p38α severely blunted CCN1/FasL-in-

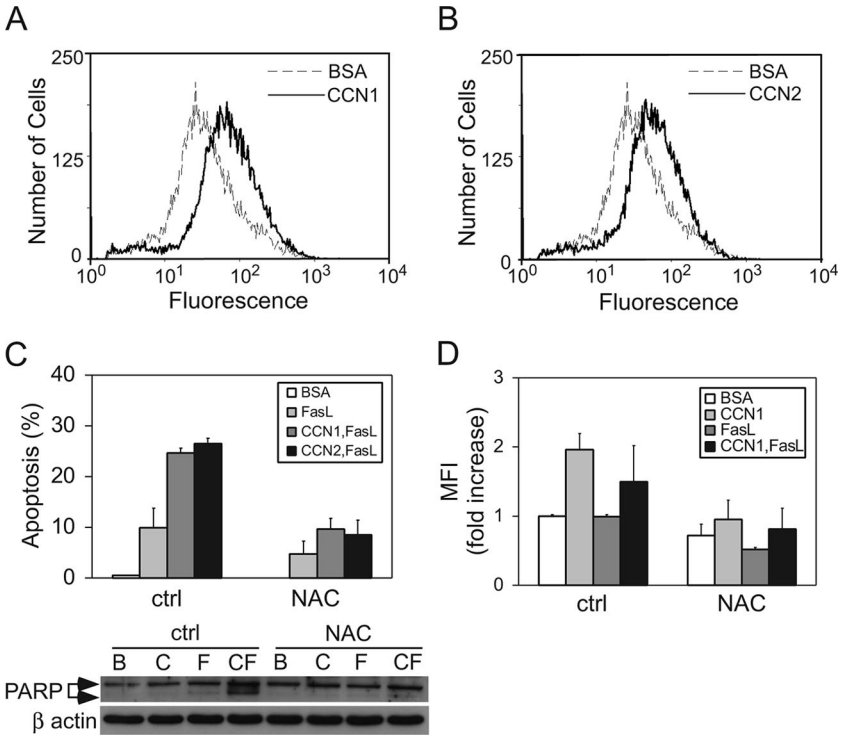


FIG. 4. CCN1- and CCN2-induced ROS are essential for their synergism with FasL. (A and B) Cellular levels of ROS were detected by flow cytometry in HSFs loaded with 5 μM CM-$H_2$DCFDA and treated with 2 μg/ml of CCN1 (A) or CCN2 (B). Histogram overlays show fluorescence intensity in BSA-treated control cells and cells treated with CCN1 or CCN2. (C, top) Apoptosis in cells treated for 4 h with FasL and CCN1 or CCN2, with or without preincubation with 10 mM NAC. (Bottom) Immunoblot detection of PARP cleavage in lysates of cells treated as indicated (B, BSA; C, CCN1; F, FasL; CF, CCN1 and FasL), with or without NAC preincubation. The experiment was done at least three times with similar results. (D) ROS levels in cells treated with FasL and/or CCN1, in the presence or absence of 10 mM NAC, were determined by flow cytometry. Experiments were done in triplicate, and the geometric mean fluorescence intensity (MFI) ± SD was expressed as the increase over the BSA-treated control.

duced apoptosis, indicating that p38α MAPK plays a critical role in this process (Fig. 6D, bottom).

CCN1 significantly enhanced the activation of p38 MAPK by FasL without activating p38 by itself, as judged by immunodetection of dual phosphorylation on Thr-180/Tyr-182 (Fig. 6E). Hyperphosphorylation of p38 MAPK by CCN1/FasL treatment is ROS dependent, since it was blocked by NAC (Fig. 6E). This result prompted us to postulate that CCN1-induced ROS generation through nSMase1 may be critical for p38 MAPK hyperphosphorylation. Both knockdown of nSMase1 expression by siRNA and treatment of cells with the nSMase inhibitor GW4869 greatly diminished CCN1/FasL-induced p38 MAPK phosphorylation, showing that redox-sensitive hyperphosphorylation of p38 MAPK is indeed dependent on nSMase1 (Fig. 6F).

Next we assessed the importance of the mitochondria in CCN1/FasL synergism. We found that overexpression of Bcl-2, an antiapoptotic protein known to block all mitochondrial apoptogenic activity (33), was sufficient to completely abolish apoptosis induced by FasL and CCN1/FasL (Fig. 7A). Thus, both FasL and CCN1/FasL synergism require mitochondrial participation to induce apoptosis. Since p38 MAPK contributes to several apoptotic pathways by regulating the translocation of the proapoptotic protein Bax from cytosol to mitochondria to trigger cytochrome *c* release (23), we monitored cytochrome *c* release by immunostaining (Fig. 7B, top) and subcellular fractionation (Fig. 7B, bottom). Stimulation of cells with CCN1 and FasL triggered a massive release of cytochrome *c* to the cytoplasm compared to treatment with FasL alone (Fig. 7B, bottom). The synergistic effect of CCN1/FasL on cytochrome *c* release was completely blocked by SB203580, indicating its dependence on p38 MAPK. We also assessed the subcellular localization of Bax by immunocytochemistry using the monoclonal anti-Bax antibody 6A7, which recognizes an N-terminal epitope that is exposed after Bax activation (Fig. 7C) (51). When MAb 6A7 was used, a large number of cells showed the presence of activated Bax localized to the mitochondria in cells treated with CCN1 and FasL. The number of cells positive for activated Bax was greatly reduced by SB203580, indicating that p38 MAPK augments cytochrome *c* release through Bax activation (Fig. 7C). Together, these results show that nSMase1 is critical for CCN1-induced ROS accumulation, leading to hyperactivation of p38 MAPK and enhanced cytochrome *c* release in the presence of FasL, resulting in synergistic apoptosis.

**CCN1 regulates Fas-induced apoptosis in vivo.** Since *Ccn1*-null mice are embryonic lethal, we turned to mice expressing mutant CCN1 to test the role of CCN1 in Fas-mediated apoptosis in vivo. For this purpose, we employed $Ccn1^{dm/dm}$ knock-in mice, in which the *Ccn1* genomic locus has been replaced by an allele encoding DM, a mutant defective for binding $\alpha_6\beta_1$-HSPG and therefore completely unable to syn-

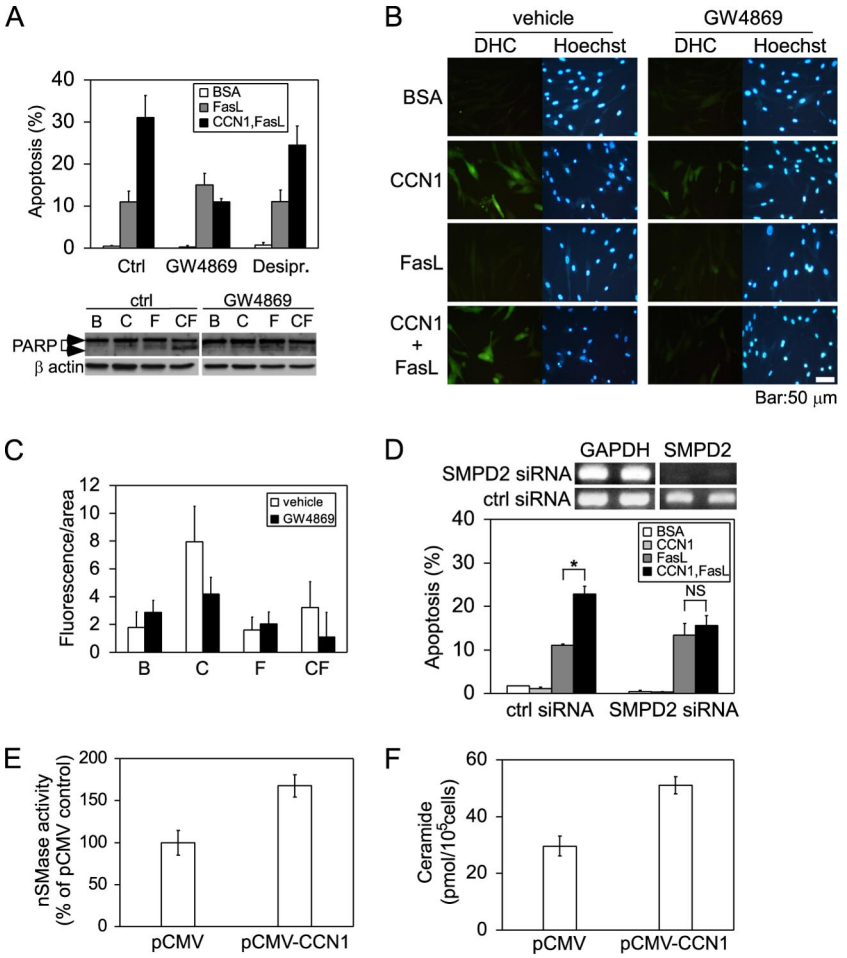


FIG. 5. nSMase is essential for CCN1-induced ROS accumulation and synergism with FasL. (A, top) Apoptosis in HSFs that were either untreated (ctrl) or incubated with GW4869 (20 μM) or desipramine (25 μM) before addition of FasL and CCN1. (Bottom) Immunoblot detection of PARP cleavage in lysates of cells treated as indicated (B, BSA; C, CCN1; F, FasL; CF, CCN1 and FasL), with or without preincubation with GW4869. (B) After preincubation with 20 μM GW4869 or vehicle (1.3% dimethyl sulfoxide), cells were treated with CCN1 and/or FasL for 2 h and loaded with DHC for fluorescence microscopy. (C) Five randomly selected high-power microscopic fields of cells/sample, treated as above, were photographed, and the average fluorescence intensity was analyzed using ImageJ software and presented as mean ± SD. (D) HSFs were transfected with either SMPD2 (nSMase1) or control siRNA. Expression of SMPD2 and GAPDH was determined after 72 h using semiquantitative RT-PCR (top; duplicate samples). Transfected cells were treated with CCN1 and/or FasL, and apoptosis was scored (bottom). Data represent the means ± SD of an experiment done in triplicate (*, $P < 0.05$; NS, not significant). (E) nSMase activity was measured 24 h after transfection of HSFs with the pCMV-CCN1 construct or an empty vector (pCMV). Results are presented as % of vector-transfected control ± SD obtained from three independent experiments. (F) Ceramide levels in HSFs were determined by diacylglycerol kinase assay 24 h after transfection with either an empty vector or pCMV-CCN1.

ergize with FasL (Fig. 2D) (10). *Ccn1*$^{dm/dm}$ mice are viable and fertile and exhibit no overt morphological or behavioral defects. We isolated MEFs from *Ccn1*$^{dm/dm}$ mice and found that they showed reduced sensitivity to FasL-induced cell death compared to wild-type MEFs, responding only at very high concentrations of FasL (Fig. 8A). Intracellular peroxide and superoxide levels in *Ccn1*$^{dm/dm}$ MEFs were significantly lower than those in wild-type MEFs (Fig. 8B), showing that endogenously expressed CCN1 plays an important role in cellular ROS generation.

In addition to lymphocytes, Fas mediates apoptosis in many nonlymphoid tissues in the organism upon inflammation and injury (19). Systemic administration of the agonistic anti-Fas MAb Jo2 causes massive hepatic apoptosis and liver hemorrhage and serves as a model to examine Fas-specific apoptosis in vivo (52). We delivered Jo2 intravenously into wild-type and *Ccn1*$^{dm/dm}$ knock-in mice and analyzed hepatic apoptosis 2 h later by TUNEL assay (Fig. 9A). Whereas Jo2 elicited substantial hepatic cell death in wild-type mice, Fas-dependent apoptosis was suppressed by >65% in *Ccn1*$^{dm/dm}$ mice (Fig. 7B). By contrast, injection of control IgG did not result in any detectable hepatic apoptosis. Two independent lines of *Ccn1*$^{dm/dm}$ mice showed comparable results. Consistent with a reduced level of apoptotic liver damage, the serum ALT levels measured after Jo2 delivery were significantly lower in *Ccn1*$^{dm/dm}$ mice than in wild-type mice, whereas control mice of either genotype had barely detectable ALT levels (Fig. 9C). The specificity of the Jo2 MAb and the *Ccn1*$^{dm}$ mutation allows us to conclude that Fas-mediated apoptosis is critically dependent on CCN1 functions in vivo.

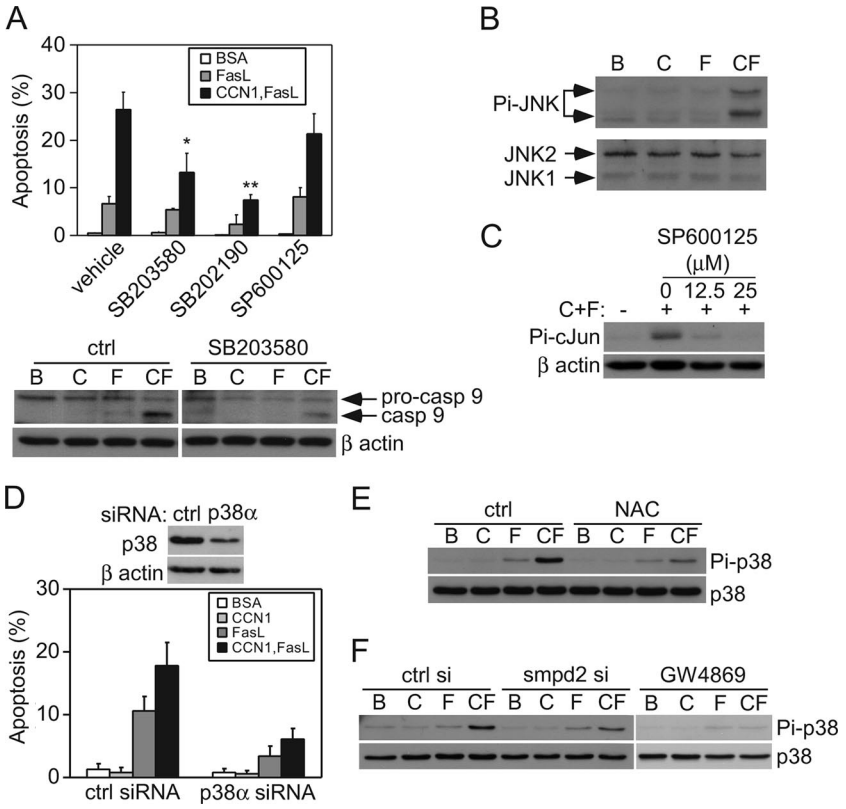


FIG. 6. ROS-dependent hyperactivation of p38 MAPK is critical for FasL/CCN1-induced apoptosis. (A, top) Apoptosis of HSFs treated with vehicle (dimethyl sulfoxide), the p38 MAPK inhibitor SB203580 or SB202190 (10 μM each), or the JNK inhibitor SP600125 (12 μM) prior to stimulation with FasL with or without CCN1. *, $P < 0.05$; **, $P < 0.01$. (Bottom) Immunoblot analysis of caspase-9 processing in lysates of cells treated as indicated (B, BSA; C, CCN1; F, FasL; CF, CCN1 and FasL), with or without preincubation with 40 μM SB203580. (B) HSFs were treated with various proteins, and total cell lysates, collected after 4 h of incubation, were analyzed for phospho-JNK1/2 (Pi-JNK; Thr183/Tyr185) and total JNK1/2 by immunoblotting. (C) HSFs were pretreated with various concentrations of SP600125 for 1 h and left uninduced or induced with CCN1 and FasL (C+F) for 4 h. Whole-cell lysates were immunoblotted against phospho-c-Jun (Ser63) and β-actin. (D, top) Lysates from cells transfected with control or p38α siRNA were immunoblotted with antibodies against p38 MAPK and β-actin. (Bottom) Transfected cells were stimulated with CCN1 and/or FasL; apoptosis was scored 4 h thereafter. (E) HSFs were treated as indicated in the presence or absence of NAC. After 4 h, total lysates were collected and analyzed for phospho-p38 MAPK (Thr180/Tyr182) and total p38 by immunoblotting. (F) Cells transfected with control or SMPD2 siRNA or treated with the nSMase inhibitor GW4869 (20 μM) were stimulated with CCN1 and/or FasL as described above. Cell lysates were immunoblotted for phosphorylated and total p38.

To assess the role of CCN1 in Fas-mediated apoptosis under physiologic conditions further, we employed an alcohol-induced-apoptosis model. It has been shown that the intake of a single bolus of alcohol in mice results in Fas-dependent hepatic apoptosis, an effect that is eliminated by intravenous delivery of a neutralizing anti-FasL antibody (70). Therefore, we treated wild-type and *Ccn1*$^{dm/dm}$ mice with a single dose of alcohol intragastrically and examined liver apoptosis 24 h thereafter. Hepatic apoptosis was reduced by 60 to 70% in *Ccn1*$^{dm/dm}$ mice compared to wild-type mice, indicating that physiologic cell death mediated through Fas is regulated by CCN1 (Fig. 9D). Together, these results show that the matricellular protein CCN1 in the ECM microenvironment acts as a contextual regulator of physiologic Fas-mediated apoptosis.

## DISCUSSION

The present study provides new insights into how Fas-mediated apoptosis may be regulated in a context-dependent manner by the ECM microenvironment. In addition to the deletion of activated T and B cells and the suppression of inflammation in immune-privileged tissues, FasL also induces apoptosis in parenchymal cells of many nonlymphoid tissues through its broadly expressed receptor Fas upon injury and inflammatory infiltration of lymphocytes (20, 42, 46). Our study shows that the matricellular proteins CCN1 and CCN2, which are highly expressed in wounded and inflamed tissues, significantly synergize with Fas-mediated apoptosis through integrin-dependent redox signaling. Furthermore, Fas-mediated apoptosis is severely blunted in knock-in mice expressing a *Ccn1* allele encoding an $\alpha_6\beta_1$-HSPG-binding-defective protein. These results demonstrate that the cellular response to Fas-mediated apoptosis is regulated by the ECM milieu through the expression of CCN matricellular proteins.

Cell adhesion to the ECM typically induces integrin signaling and invokes cytoprotective functions against numerous proapoptotic stimuli, including serum withdrawal, cytokines, chemotherapeutic agents, and loss of cell adhesion (13). Mechanistically, ligation of integrins activates focal adhesion kinase, integrin-linked kinase, and Src kinases, resulting in signals

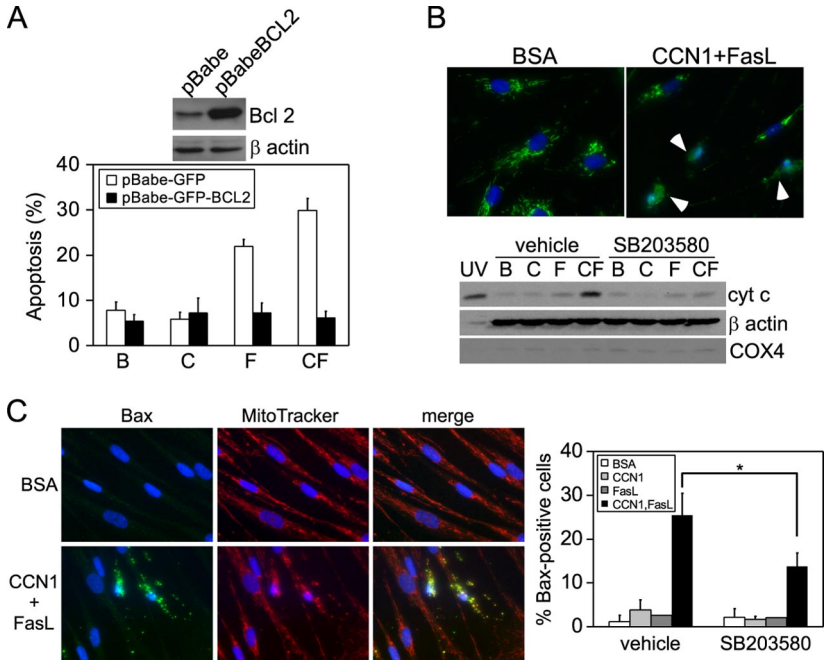


FIG. 7. CCN1 augments Fas apoptosis by p38 MAPK-dependent Bax activation and mitochondrial cytochrome *c* release. (A, top) Lysates of cells transfected with empty vector (pBabe) or a Bcl 2 overexpression construct (pBabe-BCL2) were immunoblotted against Bcl 2 or β-actin as a loading control. (Bottom) Apoptotic index in GFP-positive transfectants 5 h after treatment with factors as indicated (B, BSA; C, CCN1; F, FasL; CF, CCN1 and FasL). (B, top) HSFs grown on chamber slides were serum starved prior to treatment with CCN1 and FasL. Cytochrome *c* was detected by immunofluorescence staining using anti-cytochrome *c* MAb (6H2.B4) followed by Alexa Fluor 488-conjugated secondary antibody (green). Nuclei were counterstained with DAPI (blue). Arrowheads point to cytochrome *c* released to cytoplasm. Magnification, ×400. (Bottom) HSFs were preincubated with the p38 inhibitor SB203580 (40 μM) or vehicle (dimethyl sulfoxide [DMSO]) and stimulated with CCN1 and/or FasL for 3 h. The cytosolic fractions were analyzed for cytochrome *c*, β-actin, and mitochondrial marker cytochrome *c* oxidase 4 (COX4) by immunoblotting. UV-irradiated cells were used as a control for cytochrome *c* release. (C, left) Cells were treated as indicated, and Bax was detected by immunofluorescence using the 6A7 antibody. Bax (green) and mitochondrial (red) signals were superimposed with DAPI (blue), and merged images reveal Bax and mitochondrial colocalization (yellow). Magnification, ×400. (Right) HSFs were preincubated with the p38 inhibitor SB203580 (40 μM) or vehicle (DMSO) and stimulated with CCN1 and/or FasL for 4 h. Bax-positive cells from approximately 100 cells/sample in five randomly chosen fields were counted, and triplicate treatments are presented as means ± SD (*, $P < 0.05$).

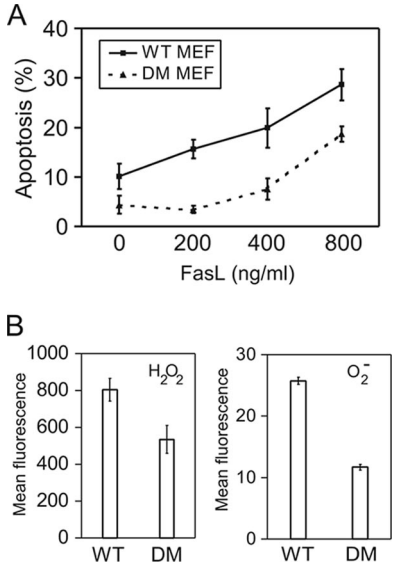


FIG. 8. MEFs from *Ccn1*$^{dm/dm}$ mice show reduced sensitivity to FasL-induced apoptosis and lower levels of ROS. (A) MEFs from wild-type (WT) or *Ccn1*$^{dm/dm}$ (DM) mice were treated with FasL in serum-free media, and apoptosis was scored after 6 h by DAPI staining. (B) Wild-type and *Ccn1*$^{dm/dm}$ MEFs were labeled with ROS indicator dye CM-$H_2$DCFDA for peroxide ($H_2O_2$) or DHE for superoxide ($O_2^-$). Fluorescence intensity was detected by flow cytometry.

transduced downstream to phosphatidylinositol 3-kinase/Akt and MAPK survival pathways. Indeed, ligation of integrin $\alpha_2\beta_1$ or $\alpha_5\beta_1$ inhibits Fas-mediated apoptosis in T lymphocytes or synovial cells, respectively (22, 32). Contradictory to the notion that cell adhesion promotes cell survival, a group of ECM proteins that can induce apoptosis has recently begun to emerge. For example, whereas CCN1 and CCN2 promote survival in endothelial cells through binding to integrin $\alpha_v\beta_3$, they can also induce apoptosis in fibroblasts through the engagement of $\alpha_6\beta_1$-HSPGs (40, 60). Likewise, other ECM proteins, including thrombospondin-1 and EMILIN-2, have been reported to induce apoptosis through upregulation of FasL expression or activation of the death receptor DR-4, respectively (49, 65). This study shows that the presence of CCN matricellular proteins can profoundly regulate Fas-mediated apoptosis, thereby adding another layer of complexity to the contextual control of cell death and survival by the ECM.

CCN1/FasL-induced apoptosis occurs with rapid kinetics within 4 to 6 h and is independent of de novo protein synthesis. CCN1 does not regulate Fas expression but synergizes with Fas signaling through its engagement of integrin $\alpha_6\beta_1$ and HSPGs to induce cellular ROS accumulation, in part through nSMase1. CCN1-induced ROS produce hyperactivation of p38 MAPK and increased activation of Bax in the presence of

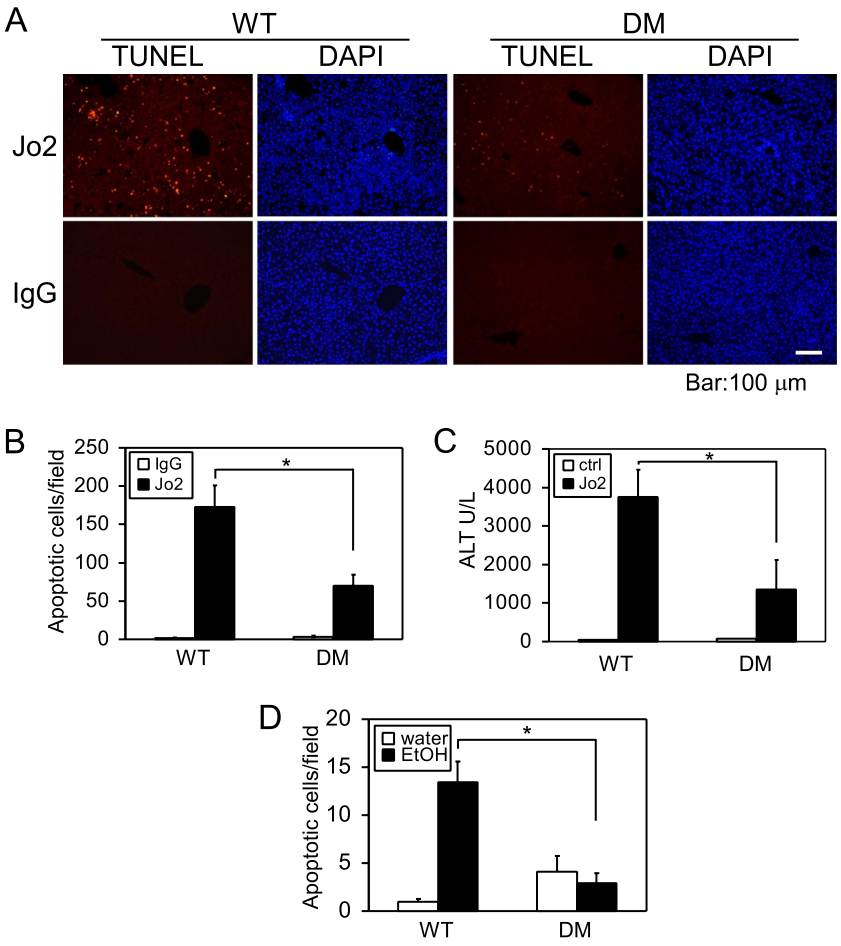


FIG. 9. *Ccn1*$^{dm/dm}$ mice are blunted in Fas-mediated apoptosis. (A) Anti-Fas MAb (Jo2) or normal hamster IgG was delivered via tail vein injection to wild-type (WT) and *Ccn1*$^{dm/dm}$ (DM) male mice, and animals were sacrificed 2 h thereafter. Apoptosis in liver sections was detected by TUNEL assay, and cells were counterstained with DAPI. (B) Apoptotic cells in Jo2-treated livers as described above in five randomly chosen fields were counted. Results are presented as means ± standard errors (SE) (WT IgG, $n = 3$; DM IgG, $n = 3$; WT Jo2, $n = 6$; DM Jo2, $n = 7$; *, $P < 0.02$ between Jo2-treated samples). Two independent *Ccn1*$^{dm/dm}$ knock-in mouse lines showed similar results. (C) Serum ALT levels in control mice or in mice 4 h after intraperitoneal delivery of Jo2 were measured. Results are presented as means ± SE (WT IgG, $n = 4$; DM IgG, $n = 4$; WT Jo2, $n = 6$; DM Jo2, $n = 7$; *, $P < 0.05$ between Jo2-treated samples). (D) Wild-type and *Ccn1*$^{dm/dm}$ male mice received alcohol by intragastric feeding, and livers were collected 24 h after treatment. Apoptosis was detected by TUNEL assay (WT water, $n = 3$; DM water, $n = 3$; WT ethanol, $n = 6$; DM ethanol, $n = 5$; *, $P < 0.005$ between ethanol-treated samples).

FasL, resulting in enhanced cytochrome *c* release and apoptosis (Fig. 7). Cytoplasmic cytochrome *c* forms the apoptosome with Apaf-1 to activate caspase-9 and consequently caspase-3, which triggers apoptosis. Activated caspase-3 may further activate caspase-8 in a positive-feedback loop, thereby amplifying the upstream caspase cascade (68). Since CCN2 is highly homologous to CCN1 and binds the same receptors, its mechanism of action is likely similar (8, 10).

The ability of CCN1 and CCN2 to induce significant ROS accumulation is central to their apoptotic synergism with FasL (Fig. 4). Indeed, wild-type MEFs accumulate more peroxides and superoxides than *Ccn1*$^{dm/dm}$ MEFs (Fig. 8B) and are more susceptible to apoptosis induction by a variety of pharmacological agents such as taxol, AN, and methyl methanesulfonate (data not shown). Our previous studies have shown that CCN1 can induce ROS accumulation through 5-lipoxygenase and the mitochondria via a Rac1-dependent mechanism (10). Indeed, inhibitors of 5-lipoxygenase or mitochondrial complex I blocked both FasL-induced and CCN1/FasL-induced apoptosis, suggesting that these mechanisms of ROS generation can contribute to Fas signaling (data not shown). Since aSMases can regulate Fas-mediated apoptosis in specific cell types (43), we investigated the potential role of SMases in CCN1/FasL-induced apoptosis. We show for the first time that CCN1 can activate nSMase activity and that nSMase1, but not aSMases, is critical for CCN1-induced ROS and synergism with FasL. This result is unexpected because nSMase has not been previously associated with apoptotic signaling and is not required for apoptosis induced by FasL alone (Fig. 5A and D). CCN1 activates the membrane-associated nSMase enzyme activity and the accumulation of ceramide (Fig. 5E and F), which, in turn, can increase cellular ROS (67). Little is known about the mechanisms of nSMase activation by extracellular signals, although the adaptor protein FAN is required for its activation by TNF-α (1). The mechanism by which ECM proteins activate nSMase is currently unknown and without precedent, whereas

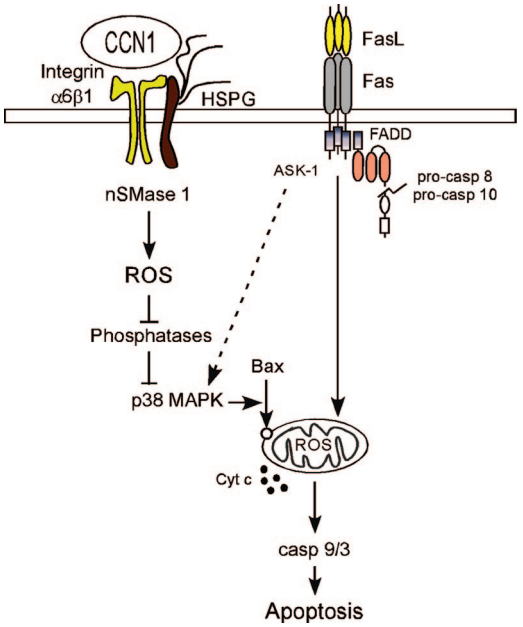


FIG. 10. Model for the signaling cross talk between CCN1 and FasL. CCN1 engages integrin $\alpha_6\beta_1$ and HSPGs to induce accumulation of cellular ROS through nSMase1. CCN1-induced ROS in the presence of FasL lead to hyperactivation of p38 MAPK, which triggers a significant increase in Bax activation, cytochrome *c* (Cyt c) release, and apoptosis.

it has been suggested that the lysosomal aSMase is negatively regulated by $\alpha_v$ integrins. Engagement of $\alpha_v\beta_3$ leads to suppression of aSMase activity and reduced apoptosis in oligodendrocytes, and blockade of $\alpha_v\beta_3/\alpha_v\beta_5$ increases ceramide accumulation and apoptosis in endothelial cells through aSMase (14, 21). Understanding how nSMase is activated through CCN1-integrin interaction will require further investigation.

A critical point of convergence between signaling induced by CCN1 and FasL is the superactivation of p38 MAPK (Fig. 10). Although CCN1 alone does not activate p38 MAPK, it greatly amplifies the effect of FasL on p38 MAPK activation in a ROS-dependent manner (Fig. 6E and F), possibly through the inhibition of phosphatases by ROS (18). Under our experimental conditions, CCN1-induced ROS are insufficient to trigger apoptosis but suffice to superactivate p38 in the presence of FasL to mediate synergism. Since CCN1/FasL synergism is independent of de novo protein synthesis, the ability of p38 MAPK to regulate transcription is not critical. Rather, hyperactivation of p38 is necessary for the activation of the proapoptotic protein Bax and its recruitment to mitochondria, thus enhancing cytochrome *c* release and apoptosis (Fig. 7). Consistent with this observation, p38 MAPK has been shown to phosphorylate and diminish the antiapoptotic activity of members of the Bcl-2 family, thereby promoting the translocation of Bax/Bak to the mitochondria (24, 61). Concordant with our finding that p38α plays a role in CCN1/FasL-induced apoptosis, MEFs and cardiomyocytes derived from $p38\alpha^{-/-}$ mice are more resistant to Jo2-induced, Fas-mediated apoptosis (55). Nevertheless, p38 MAPK can also play a prosurvival role in some cell types, suggesting that its role in apoptosis can be highly contextual (53, 69).

We conclude that CCN1 is an important regulator of Fas-mediated apoptosis in vivo based on experiments carried out using $Ccn1^{dm/dm}$ knock-in mice, which express a mutant CCN1 that is impaired for binding $\alpha_6\beta_1$-HSPG and is thus defective for apoptotic synergism with FasL. First, endogenously expressed CCN1 contributes significantly to cellular ROS production and responsiveness to FasL in MEFs (Fig. 8). Second, hepatic apoptosis induced by Jo2, an agonistic anti-Fas MAb, is severely blunted in $Ccn1^{dm/dm}$ mice (Fig. 9). Reduced hepatic injury induced by Jo2 treatment is also demonstrated by reduced levels of serum ALT in $Ccn1^{dm/dm}$ mice (Fig. 9C). Jo2 is highly specific for Fas, and Jo2-induced apoptosis is completely obliterated in the Fas-deficient *lpr* mutant mice (52). These results establish the ability of CCN1 to regulate Fas-mediated apoptosis in vivo.

In what physiological contexts might CCN1 regulate Fas-mediated apoptosis? In this study, we show that hepatic cell death is severely curtailed in $Ccn1^{dm/dm}$ mice compared to wild-type mice upon intragastric administration of alcohol (Fig. 9D), a model of binge drinking that elicits FasL-dependent hepatic apoptosis (70). Thus, the matrix microenvironment, as defined by the expression of CCN1, significantly regulates Fas-mediated apoptosis in this physiologic model. Since CCN1 expression is highly induced in many organs and tissues at sites of inflammation and wound repair, where lymphocytes infiltrate and express cytokines such as FasL, the potential interaction of CCN1 and FasL may occur in numerous circumstances of injury repair (9). For example, CCN1 is highly expressed in cardiomyocytes after myocardial infarctions and ischemic injuries (27), conditions that induce Fas-dependent cardiac apoptosis (38, 42). CCN1 is also induced upon vascular injury following balloon angioplasty and in atherosclerotic plaques (25, 58), where Fas/FasL-dependent apoptosis is observed (7, 46). The potential involvement of CCN1 in Fas-mediated cell death in these and other physiologic contexts can be tested directly in future studies using animal models such as $Ccn1^{dm/dm}$ mice or by siRNA-mediated knockdowns in vivo. Since CCN2 also synergizes with FasL, it is anticipated that double mutants that eliminate the apoptotic activity of both CCN1 and CCN2 may evoke an even stronger cytoprotective effect against Fas-mediated apoptosis than that observed in $Ccn1^{dm/dm}$ mice.

Multiple protein factors are expressed within the microenvironment of inflammation and tissue injury including TNF-α, a potent proinflammatory cytokine that induces prosurvival and antiapoptotic pathways through its strong activation of NF-κB (64). The presence of CCN1 or CCN2 turns TNF-α from being a proliferation-promoting factor in fibroblasts into an apoptotic inducer, without inhibiting NF-κB functions (10). Furthermore, the cytotoxicity of TNF-α is also dependent on CCN1 in vivo. These results and our current findings show that CCN1 and CCN2 are able to significantly modify the activities of TNF family cytokines, including FasL and TNF-α, and this interaction has been demonstrated in vivo at least for CCN1. These observations point to an unexpected interaction between members of two unrelated protein families—the CCN matricellular proteins and the TNF family of cytokines—and reveal a novel mechanism by which the ECM can modulate TNF cytokine-dependent apoptosis through the expression of CCN proteins.

## ACKNOWLEDGMENTS

We thank Nissim Hay for providing us with Bcl-2 expression vectors and Stephen Lam for a gift of anti-VNR-1 antibodies.

This work was supported by grants from the National Institutes of Health to L.F.L. (CA46565, GM78492) and a predoctoral fellowship from the American Heart Association to V. Juric.

## REFERENCES

1. **Adam-Klages, S., D. Adam, K. Wiegmann, S. Struve, W. Kolanus, J. Schneider-Mergener, and M. Kronke.** 1996. FAN, a novel WD-repeat protein, couples the p55 TNF-receptor to neutral sphingomyelinase. Cell **86:**937–947.
2. **Afzal, M., S. Matsugo, M. Sasai, B. Xu, K. Aoyama, and T. Takeuchi.** 2003. Method to overcome photoreaction, a serious drawback to the use of dichlorofluorescin in evaluation of reactive oxygen species. Biochem. Biophys. Res. Commun. **304:**619–624.
3. **Babic, A. M., C.-C. Chen, and L. F. Lau.** 1999. Fisp12/mouse connective tissue growth factor mediates endothelial cell adhesion and migration through integrin $\alpha_v\beta_3$, promotes endothelial cell survival, and induces angiogenesis in vivo. Mol. Cell. Biol. **19:**2958–2966.
4. **Baehrecke, E. H.** 2002. How death shapes life during development. Nat. Rev. Mol. Cell Biol. **3:**779–787.
5. **Bligh, E. G., and W. J. Dyer.** 1959. A rapid method of total lipid extraction and purification. Can. J. Biochem. Physiol. **37:**911–917.
6. **Bornstein, P., and E. H. Sage.** 2002. Matricellular proteins: extracellular modulators of cell function. Curr. Opin. Cell Biol. **14:**608–616.
7. **Cai, W., B. Devaux, W. Schaper, and J. Schaper.** 1997. The role of Fas/APO 1 and apoptosis in the development of human atherosclerotic lesions. Atherosclerosis **131:**177–186.
8. **Chen, C.-C., N. Chen, and L. F. Lau.** 2001. The angiogenic factors Cyr61 and CTGF induce adhesive signaling in primary human skin fibroblasts. J. Biol. Chem. **276:**10443–10452.
9. **Chen, C.-C., and L. F. Lau.** 2009. Functions and mechanisms of action of CCN matricellular proteins. Int. J. Biochem. Cell Biol. **41:**771–783.
10. **Chen, C.-C., J. L. Young, R. I. Monzon, N. Chen, V. Todorovic, and L. F. Lau.** 2007. Cytotoxicity of TNF$\alpha$ is regulated by integrin-mediated matrix signaling. EMBO J. **26:**1257–1267.
11. **Chen, N., S.-J. Leu, V. Todorovic, S. C. T. Lam, and L. F. Lau.** 2004. Identification of a novel integrin $\alpha v\beta 3$ binding site in CCN1 (CYR61) critical for pro-angiogenic activities in vascular endothelial cells. J. Biol. Chem. **279:**44166–44176.
12. **Cheresh, D. A., and D. G. Stupack.** 2008. Regulation of angiogenesis: apoptotic cues from the ECM. Oncogene **27:**6285–6298.
13. **Chiarugi, P., and E. Giannoni.** 2008. Anoikis: a necessary death program for anchorage-dependent cells. Biochem. Pharmacol. **76:**1352–1364.
14. **Chudakova, D. A., Y. H. Zeidan, B. W. Wheeler, J. Yu, S. A. Novgorodov, M. S. Kindy, Y. A. Hannun, and T. I. Gudz.** 2008. Integrin-associated Lyn kinase promotes cell survival by suppressing acid sphingomyelinase activity. J. Biol. Chem. **283:**28806–28816.
15. **Cifone, M. G., R. De Maria, P. Roncaioli, M. R. Rippo, M. Azuma, L. L. Lanier, A. Santoni, and R. Testi.** 1994. Apoptotic signaling through CD95 (Fas/Apo-1) activates an acidic sphingomyelinase. J. Exp. Med. **180:**1547–1552.
16. **Clarke, C. J., C. F. Snook, M. Tani, N. Matmati, N. Marchesini, and Y. A. Hannun.** 2006. The extended family of neutral sphingomyelinases. Biochemistry **45:**11247–11256.
17. **Coligan, J. E., A. M. Kruisbeek, D. H. Marguliees, E. M. Shevach, and W. Strober.** 1995. Related isolation procedures and functional assays, p. 3.17.2. *In* R. Coico (ed.), Current protocols in immunology, vol. 1. John Wiley & Sons, Inc., Hoboken, NJ.
18. **Cross, J. V., and D. J. Templeton.** 2006. Regulation of signal transduction through protein cysteine oxidation. Antioxid. Redox Signal. **8:**1819–1827.
19. **Curtin, J. F., and T. G. Cotter.** 2003. Live and let die: regulatory mechanisms in Fas-mediated apoptosis. Cell. Signal. **15:**983–992.
20. **DosReis, G. A., V. M. Borges, and W. A. Zin.** 2004. The central role of Fas-ligand cell signaling in inflammatory lung diseases. J. Cell. Mol. Med. **8:**285–293.
21. **Erdreich-Epstein, A., L. B. Tran, O. T. Cox, E. Y. Huang, W. E. Laug, H. Shimada, and M. Millard.** 2005. Endothelial apoptosis induced by inhibition of integrins $\alpha v\beta 3$ and $\alpha v\beta 5$ involves ceramide metabolic pathways. Blood **105:**4353–4361.
22. **Gendron, S., J. Couture, and F. Aoudjit.** 2003. Integrin $\alpha 2\beta 1$ inhibits Fas-mediated apoptosis in T lymphocytes by protein phosphatase 2A-dependent activation of the MAPK/ERK pathway. J. Biol. Chem. **278:**48633–48643.
23. **Ghatan, S., S. Larner, Y. Kinoshita, M. Hetman, L. Patel, Z. Xia, R. J. Youle, and R. S. Morrison.** 2000. p38 MAP kinase mediates bax translocation in nitric oxide-induced apoptosis in neurons. J. Cell Biol. **150:**335–347.
24. **Gomez-Lazaro, M., M. F. Galindo, R. M. Melero-Fernandez de Mera, F. J. Fernandez-Gomez, C. G. Concannon, M. F. Segura, J. X. Comella, J. H. Prehn, and J. Jordan.** 2007. Reactive oxygen species and p38 mitogen-activated protein kinase activate Bax to induce mitochondrial cytochrome c release and apoptosis in response to malonate. Mol. Pharmacol. **71:**736–743.
25. **Grzeszkiewicz, T. M., V. Lindner, N. Chen, S. C. T. Lam, and L. F. Lau.** 2002. The angiogenic factor CYR61 supports vascular smooth muscle cell adhesion and stimulates chemotaxis through integrin $\alpha 6\beta 1$ and cell surface heparan sulfate proteoglycans. Endocrinology **143:**1441–1450.
26. **Hagimoto, N., K. Kuwano, I. Inoshima, M. Yoshimi, N. Nakamura, M. Fujita, T. Maeyama, and N. Hara.** 2002. TGF-beta 1 as an enhancer of Fas-mediated apoptosis of lung epithelial cells. J. Immunol. **168:**6470–6478.
27. **Hilfiker-Kleiner, D., K. Kaminski, A. Kaminska, M. Fuchs, G. Klein, E. Podewski, K. Grote, I. Kiian, K. C. Wollert, A. Hilfiker, and H. Drexler.** 2004. Regulation of proangiogenic factor CCN1 in cardiac muscle: impact of ischemia, pressure overload, and neurohumoral activation. Circulation **109:**2227–2233.
28. **Hsu, Y. T., and R. J. Youle.** 1998. Bax in murine thymus is a soluble monomeric protein that displays differential detergent-induced conformations. J. Biol. Chem. **273:**10777–10783.
29. **Ivkovic, S., B. S. Yoon, S. N. Popoff, F. F. Safadi, D. E. Libuda, R. C. Stephenson, A. Daluiski, and K. M. Lyons.** 2003. Connective tissue growth factor coordinates chondrogenesis and angiogenesis during skeletal development. Development **130:**2779–2791.
30. **Jackson, A. L., S. R. Bartz, J. Schelter, S. V. Kobayashi, J. Burchard, M. Mao, B. Li, G. Cavet, and P. S. Linsley.** 2003. Expression profiling reveals off-target gene regulation by RNAi. Nat. Biotechnol. **21:**635–637.
31. **Kamata, H., S. Honda, S. Maeda, L. Chang, H. Hirata, and M. Karin.** 2005. Reactive oxygen species promote TNFalpha-induced death and sustained JNK activation by inhibiting MAP kinase phosphatases. Cell **120:**649–661.
32. **Kitagawa, A., Y. Miura, R. Saura, M. Mitani, H. Ishikawa, A. Hashiramoto, S. Yoshiya, S. Shiozawa, and M. Kurosaka.** 2006. Anchorage on fibronectin via VLA-5 ($\alpha 5\beta 1$ integrin) protects rheumatoid synovial cells from Fas-induced apoptosis. Ann. Rheum. Dis. **65:**721–727.
33. **Kluck, R. M., E. Bossy-Wetzel, D. R. Green, and D. D. Newmeyer.** 1997. The release of cytochrome c from mitochondria: a primary site for Bcl-2 regulation of apoptosis. Science **275:**1132–1136.
34. **Kolesnick, R.** 2002. The therapeutic potential of modulating the ceramide/sphingomyelin pathway. J. Clin. Investig. **110:**3–8.
35. **Kreuz, S., D. Siegmund, J. J. Rumpf, D. Samel, M. Leverkus, O. Janssen, G. Hacker, O. Dittrich-Breiholz, M. Kracht, P. Scheurich, and H. Wajant.** 2004. NF$\kappa$B activation by Fas is mediated through FADD, caspase-8, and RIP and is inhibited by FLIP. J. Cell Biol. **166:**369–380.
36. **Lau, L. F., and S. C. T. Lam.** 2005. Integrin-mediated CCN functions, p. 61–79. *In* B. Perbal and M. Takigawa (ed.), CCN proteins: a new family of cell growth and differentiation regulators. Imperial College Press, London, United Kingdom.
37. **Lee, K., and W. J. Esselman.** 2002. Inhibition of PTPs by $H_2O_2$ regulates the activation of distinct MAPK pathways. Free Radic. Biol. Med. **33:**1121–1132.
38. **Lee, P., M. Sata, D. J. Lefer, S. M. Factor, K. Walsh, and R. N. Kitsis.** 2003. Fas pathway is a critical mediator of cardiac myocyte death and MI during ischemia-reperfusion in vivo. Am. J. Physiol. Heart Circ. Physiol. **284:**H456–H463.
39. **Leu, S.-J., N. Chen, C.-C. Chen, V. Todorovic, T. Bai, V. Juric, Y. Liu, G. Yan, S. C. T. Lam, and L. F. Lau.** 2004. Targeted mutagenesis of the matricellular protein CCN1 (CYR61): selective inactivation of integrin $\alpha 6\beta 1$-heparan sulfate proteoglycan coreceptor-mediated cellular activities. J. Biol. Chem. **279:**44177–44187.
40. **Leu, S.-J., S. C. T. Lam, and L. F. Lau.** 2002. Proangiogenic activities of CYR61 (CCN1) mediated through integrins $\alpha v\beta 3$ and $\alpha 6\beta 1$ in human umbilical vein endothelial cells. J. Biol. Chem. **277:**46248–46255.
41. **Li, J., and J. Yuan.** 2008. Caspases in apoptosis and beyond. Oncogene **27:**6194–6206.
42. **Li, Y., G. Takemura, K. Kosai, T. Takahashi, H. Okada, S. Miyata, K. Yuge, S. Nagano, M. Esaki, N. C. Khai, K. Goto, A. Mikami, R. Maruyama, S. Minatoguchi, T. Fujiwara, and H. Fujiwara.** 2004. Critical roles for the Fas/Fas ligand system in postinfarction ventricular remodeling and heart failure. Circ. Res. **95:**627–636.
43. **Lin, T., L. Genestier, M. J. Pinkoski, A. Castro, S. Nicholas, R. Mogil, F. Paris, Z. Fuks, E. H. Schuchman, R. N. Kolesnick, and D. R. Green.** 2000. Role of acidic sphingomyelinase in Fas/CD95-mediated cell death. J. Biol. Chem. **275:**8657–8663.
44. **Low, W., A. Smith, A. Ashworth, and M. Collins.** 1999. JNK activation is not required for Fas-mediated apoptosis. Oncogene **18:**3737–3741.
45. **Majewski, N., V. Nogueira, P. Bhaskar, P. E. Coy, J. E. Skeen, K. Gottlob, N. S. Chandel, C. B. Thompson, R. B. Robey, and N. Hay.** 2004. Hexokinase-mitochondria interaction mediated by Akt is required to inhibit apoptosis in the presence or absence of Bax and Bak. Mol. Cell **16:**819–830.
46. **Matter, C. M., C. E. Chadjichristos, P. Meier, T. von Lukowicz, C. Lohmann, P. K. Schuler, D. Zhang, B. Odermatt, E. Hofmann, T. Brunner, B. R. Kwak, and T. F. Luscher.** 2006. Role of endogenous Fas (CD95/Apo-1) ligand in balloon-induced apoptosis, inflammation, and neointima formation. Circulation **113:**1879–1887.
47. **Mo, F. E., A. G. Muntean, C. C. Chen, D. B. Stolz, S. C. Watkins, and L. F.**

**Lau.** 2002. CYR61 (CCN1) is essential for placental development and vascular integrity. Mol. Cell. Biol. **22:**8709–8720.
48. **Mo, F.-E., and L. F. Lau.** 2006. The matricellular protein CCN1 is essential for cardiac development. Circ. Res. **99:**961–969.
49. **Mongiat, M., G. Ligresti, S. Marastoni, E. Lorenzon, R. Doliana, and A. Colombatti.** 2007. Regulation of the extrinsic apoptotic pathway by the extracellular matrix glycoprotein EMILIN2. Mol. Cell. Biol. **27:**7176–7187.
50. **Nagata, S.** 1999. Fas ligand-induced apoptosis. Annu. Rev. Genet. **33:**29–55.
51. **Nechushtan, A., C. L. Smith, Y. T. Hsu, and R. J. Youle.** 1999. Conformation of the Bax C-terminus regulates subcellular location and cell death. EMBO J. **18:**2330–2341.
52. **Ogasawara, J., R. Watanabe-Fukunaga, M. Adachi, A. Matsuzawa, T. Kasugai, Y. Kitamura, N. Itoh, T. Suda, and S. Nagata.** 1993. Lethal effect of the anti-Fas antibody in mice. Nature **364:**806–809.
53. **Park, J. G., Y. Yuk, H. Rhim, S. Y. Yi, and Y. S. Yoo.** 2002. Role of p38 MAPK in the regulation of apoptosis signaling induced by TNF-alpha in differentiated PC12 cells. J. Biochem. Mol. Biol. **35:**267–272.
54. **Pham, C. G., C. Bubici, F. Zazzeroni, S. Papa, J. Jones, K. Alvarez, S. Jayawardena, E. De Smaele, R. Cong, C. Beaumont, F. M. Torti, S. V. Torti, and G. Franzoso.** 2004. Ferritin heavy chain upregulation by NF-κB inhibits TNFα-induced apoptosis by suppressing reactive oxygen species. Cell **119:**529–542.
55. **Porras, A., S. Zuluaga, E. Black, A. Valladares, A. M. Alvarez, C. Ambrosino, M. Benito, and A. R. Nebreda.** 2004. P38 alpha mitogen-activated protein kinase sensitizes cells to apoptosis induced by different stimuli. Mol. Biol. Cell **15:**922–933.
56. **Preiss, J., C. R. Loomis, W. R. Bishop, R. Stein, J. E. Niedel, and R. M. Bell.** 1986. Quantitative measurement of sn-1,2-diacylglycerols present in platelets, hepatocytes, and ras- and sis-transformed normal rat kidney cells. J. Biol. Chem. **261:**8597–8600.
57. **Santiago, B., M. Galindo, G. Palao, and J. L. Pablos.** 2004. Intracellular regulation of Fas-induced apoptosis in human fibroblasts by extracellular factors and cycloheximide. J. Immunol. **172:**560–566.
58. **Schober, J. M., N. Chen, T. M. Grzeszkiewicz, E. E. Emeson, T. P. Ugarova, R. D. Ye, L. F. Lau, and S. C. T. Lam.** 2002. Identification of integrin αMβ2 as an adhesion receptor on peripheral blood moncytes for Cyr61 (CCN1) and connective tissue growth factor (CCN2), immediate-early gene products expressed in atherosclerotic lesions. Blood **99:**4457–4465.
59. **Tewari, M., L. T. Quan, K. O'Rourke, S. Desnoyers, Z. Zeng, D. R. Beidler, G. G. Poirier, G. S. Salvesen, and V. M. Dixit.** 1995. Yama/CPP32 beta, a mammalian homolog of CED-3, is a CrmA-inhibitable protease that cleaves the death substrate poly(ADP-ribose) polymerase. Cell **81:**801–809.
60. **Todorovicç, V., C.-C. Chen, N. Hay, and L. F. Lau.** 2005. The matrix protein CCN1 (CYR61) induces apoptosis in fibroblasts. J. Cell Biol. **171:**559–568.
61. **Torcia, M., G. De Chiara, L. Nencioni, S. Ammendola, D. Labardi, M. Lucibello, P. Rosini, L. N. Marlier, P. Bonini, P. Dello Sbarba, A. T. Palamara, N. Zambrano, T. Russo, E. Garaci, and F. Cozzolino.** 2001. Nerve growth factor inhibits apoptosis in memory B lymphocytes via inactivation of p38 MAPK, prevention of Bcl-2 phosphorylation, and cytochrome c release. J. Biol. Chem. **276:**39027–39036.
62. **Ubezio, P., and F. Civoli.** 1994. Flow cytometric detection of hydrogen peroxide production induced by doxorubicin in cancer cells. Free Radic. Biol. Med. **16:**509–516.
63. **Um, H. D., J. M. Orenstein, and S. M. Wahl.** 1996. Fas mediates apoptosis in human monocytes by a reactive oxygen intermediate dependent pathway. J. Immunol. **156:**3469–3477.
64. **Varfolomeev, E. E., and A. Ashkenazi.** 2004. Tumor necrosis factor: an apoptosis JuNKie? Cell **116:**491–497.
65. **Volpert, O. V., T. Zaichuk, W. Zhou, F. Reiher, T. A. Ferguson, P. M. Stuart, M. Amin, and N. P. Bouck.** 2002. Inducer-stimulated Fas targets activated endothelium for destruction by anti-angiogenic thrombospondin-1 and pigment epithelium-derived factor. Nat. Med. **8:**349–357.
66. **Wiegmann, K., S. Schutze, T. Machleidt, D. Witte, and M. Kronke.** 1994. Functional dichotomy of neutral and acidic sphingomyelinases in tumor necrosis factor signaling. Cell **78:**1005–1015.
67. **Won, J. S., and I. Singh.** 2006. Sphingolipid signaling and redox regulation. Free Radic. Biol. Med. **40:**1875–1888.
68. **Yang, S., A. D. Thor, S. Edgerton, and X. Yang.** 2006. Caspase-3 mediated feedback activation of apical caspases in doxorubicin and TNF-alpha induced apoptosis. Apoptosis **11:**1987–1997.
69. **Zechner, D., R. Craig, D. S. Hanford, P. M. McDonough, R. A. Sabbadini, and C. C. Glembotski.** 1998. MKK6 activates myocardial cell NF-κB and inhibits apoptosis in a p38 mitogen-activated protein kinase-dependent manner. J. Biol. Chem. **273:**8232–8239.
70. **Zhou, Z., X. Sun, and Y. J. Kang.** 2001. Ethanol-induced apoptosis in mouse liver: Fas- and cytochrome c-mediated caspase-3 activation pathway. Am. J. Pathol. **159:**329–338.